Publié dans Bulletin du Centre d'Hydrogéologie de
l'Université de Neuchâtel n° 15, pp. 77-98, 1998,
source qui doit être utilisée pour toute référence à ce travail

Modelling karst aquifers by the combined discrete channel and continuum approach

*Laszlo Kiraly**

ABSTRACT

The organized heterogeneity of many karst aquifers may be schematized by a high conductivity, generally unknown channel network with kilometer wide "meshes", which is "immersed" in a low conductivity fractured limestone volume, and is well connected to a local discharge area, the karst spring. The modelling of this kind of karstic structure would nearly always require the combination of the continuum approach with the discrete channel model.

As the available data on real karst channel networks are very limited, the combined approach is not widely used in applied karst hydrogeology. It represents, however, a powerful tool for checking the adequacy of the interpretation schemes based on a simpler representation of karst aquifers, where the karst channel network does not appear explicitly (global methods based on black-box or "grey-box" models, simple continuum or double continuum approach, etc.). A few examples using 2-D or 3-D finite element models are presented in this paper.

RESUME

L'hétérogénéité organisée des aquifères karstiques peut être schématisée par un réseau de conduits, très perméables, à maille kilométrique, généralement inconnu et bien relié au point de décharge (la source karstique). Le réseau est « immergé » dans un volume de calcaires fissurés peu perméables. La modélisation d'une telle structure karstique nécessite pratiquement toujours une approche combinée englobant un milieu continu et un réseau de conduits discrets.

Les données disponibles sur les caractéristiques des conduits sont généralement très limitées, ce qui explique que cette approche combinée ne soit pas largement utilisée en hydrologéologie karstique. Elle représente cependant un outil performant pour évaluer l'adéquation entre certains schémas interprétatifs basés sur des représentations simplifiées des systèmes karstiques, dans lesquelles le réseau karstique n'apparaît pas explicitement (p. ex. les approches globales basées sur des modèles boîte noire ou boîte grise, les approches à un ou deux milieux continus équivalents, etc.). Quelques exemples de modèles 2-D et 3-D à éléments finis sont présentés dans cet article.

---

* Centre d'Hydrogéologie, Université de Neuchâtel, Emile-Argand 11, CH-2007 Neuchâtel

1. Introduction and aims

1.1. Duality of karst aquifers

The reconstruction of a regional groundwater flow field, which is consistent with a given hydraulic conductivity field and with given boundary conditions, nearly always requires the use of numerical models. This is the case in karst systems where the hydraulic conductivity field and boundary conditions are particularly heterogeneous.

The organized heterogeneity of many karst aquifers may be schematized by a high permeability, generally unknown channel network with kilometer wide "meshes", which is "immersed" in a low permeability fractured limestone volume, and is well connected to a local discharge area, the karst spring. The duality of karst aquifers is a direct consequence of this structure:

- duality of the infiltration processes (diffuse or slow infiltration into the low permeability volumes, concentrated or rapid infiltration into the channel network);
- duality of the groundwater flow field (low flow velocities in the fractured volumes, high flow velocities in the channel network);
- duality of the discharge conditions (diffuse seepage from the low permeability volumes, concentrated discharge from the channel network at the karst springs).

Note that besides the rivers disappearing in swallowholes, the concentrated infiltrations could be enhanced by the rapid drainage in a high conductivity "skin" at shallow depth: the epikarst defined by MANGIN (1975).

The behaviour of the karst spring (hydrograph, chemical or isotopic composition, etc.) represents the global response of the karst aquifer to input events. As the available data on the hydraulic parameters are very limited, the global response, which is easier to measure, is often used to make hypotheses and inferences (sometimes even contradictory inferences) on the infiltration and groundwater flow processes, on the hydraulic parameter fields, as well as on the role of the low conductivity volumes, the high conductivity karst channels and the epikarst zone. The direct verification of the hypotheses or inferences by field measurements is, obviously, very difficult.

An indirect method of verification would consist in introducing the inferred karstic structures into a deterministic numerical model and then simulate their effect on the global response of the aquifer (for example, the spring hydrograph), on the groundwater flow field, on the hydraulic head distribution, etc. The simulated behaviour of the theoretical aquifer could then be compared to the usually accepted ideas on the groundwater flow processes in karst aquifers. This is the way followed by the research team of the Centre d'Hydrogéologie de l'Université de Neuchâtel (CHYN) for years.

The aim of this paper is to present the effect of the karst channel network and the epikarst zone on groundwater flow processes, as obtained by numerical finite element models simulating a few "theoretical" and oversimplified karst aquifers. The results, although theoretical, have important practical consequences on the monitoring strategies applied for

karst aquifers, on the interpretation of the global responses obtained at karst springs and on the estimation of the recharge of the low conductivity "capacitive" volumes. They suggest to ask such fundamental questions as: what is the meaning of "groundwater level" observations in boreholes when separated from hydraulic conductivity measurements; what is the meaning of the "groundwater table" represented by isolines (equipotentials) in karst aquifers; what is the hydraulic meaning of the "components" obtained by chemical or isotopic hydrograph separation methods; etc.

1.2. Combined discrete channel and continuum approach by using finite element models

In consolidated carbonate rocks, discontinuities exist at all scales and their lateral extent varies from a few centimeters (microfractures) to tens of kilometers (geological fault zones and karst channels). It seems reasonable to represent these discontinuities as networks of different orders of magnitude which are "embedded" in each other. This "nested model" concept of the geological discontinuities explains, for example, the duality of karst and the well known scale effect on the hydraulic conductivities in fractured and karstified limestone aquifers (KIRALY 1975).

The modelling of this kind of nested structures nearly always requires the combination of the continuum approach with the discrete fracture or discrete channel model. At a regional scale, for example, the discrete fracture (or channel) model alone could not be realized at all, because of the tremendous amount of discontinuities (of different orders of magnitude) which ought to be introduced into the model. On the other hand, the equivalent continuum approach alone would not show the effect of the regional fault zones or the regionally developed karst networks on the groundwater flow systems. So it seems reasonable to model the regional faults or karst networks by 2-D or 1-D "discrete" zones, whereas the volumes between them (which contain only lower order fractures or channels) might be modelled by a 3-D equivalent continuum. As a matter of fact, every discontinuity, which is "big" with respect to the size of the modelled region, should be represented by a discrete zone.

Numerical models using the finite element method are excellent for the combined discrete channel (or discrete fracture) and continuum approach, particularly if they allow for the combination of 1-D, 2-D and 3-D finite elements, as it was proposed by KIRALY (1979, 1985, 1988), KIRALY *et al.* (1995) and HELMIG (1993). In this case, the high conductivity karst channel network is simulated by 1-D linear or quadratic finite elements, which are "immersed" between 2-D or 3-D linear or quadratic elements representing the low conductivity fractured limestone volumes.

The simulations presented in this paper were carried out by the computer codes developed at the Centre d'Hydrogéologie de Neuchâtel. They simulate steady-state and transient, one-, two- or three-dimensional saturated groundwater flow by the finite element method (codes FEN1 and FEN2). The computer programs allow for the incorporation of one-, two- or three-dimensional linear or quadratic elements within a three-dimensional network. The saturated, constant density, transient groundwater flow is represented by equation (1):

$$S_s \frac{\partial h}{\partial t} + div\left(-[K]\,\overrightarrow{grad}\ h\right) + Q = 0 \qquad (1)$$

where S_s is the specific storage coefficient, $[K]$ is the hydraulic conductivity tensor, h is the hydraulic head and Q represents the general source/sink terms (infiltration, well discharges, etc.).

The formulation for the finite elements is based on the Galerkin weighted residual approach and the resulting system of linear equations is solved by the frontal elimination technique of IRONS (1970). The time dependent problem is solved in FEN2 by using the robust Crank-Nicholson implicit time-stepping scheme. UFEN1 is a code derived from FEN1 and simulates saturated/unsaturated steady-state groundwater flow. In this paper it is used to simulate the free groundwater table in a theoretical "shallow" karst aquifer. The computer codes allow the modeller to "concatenate" several aquifers into one model and this facility is used to link the epikarst with the mean aquifer.

A slightly modified version of FEN2 offers another facility when used to simulate karst aquifers. By giving the identification number of the nodal points located on the karst channels, the program calculates the flow contribution of each 3-D element (i.e. low conductivity fractured volume) to the karst net. The sum of these contributions is simply the **baseflow** which can be compared to the total spring hydrograph.

Using the linear Darcy's law to simulate the groundwater flow in saturated karst channels represents only a crude approximation of the real system, but our aim was to obtain a rapid and rather "qualitative" indication on the effect of the enormous contrast between the hydraulic conductivities of fractured limestones (10^{-6} m/s) and karst channels (10 m/s or more). The conclusions presented in this paper will not be changed qualitatively with the simulation of turbulent flow: the effects due to concentrated infiltration into the channel network (inversion of gradients, negative baseflow, etc.), for example, will be only increased.

Simulating turbulent flow in the karst channel network is an emerging activity in karst hydrogeology (WOLLRATH & HELMIG 1991; TRÖSCH & ZURBRÜGG 1995; JEANNIN & MARÉCHAL 1995), but it is not yet applied at a basin-wide scale.

2. Presentation and discussion of the results

2.1. A brief historical review

In the 1960s, modelling of karst aquifers was reduced to using multi-reservoir "grey-box" models for the simulation of karst spring hydrographs, or electric analogs based on a single continuum approach (BEDINGER 1966, TRIPET 1972) for the simulation of hydraulic heads. In the early 1970s the emerging mathematical models replaced the electric analogs, but the global "grey-box" models remained very popular until recently. The models based on the method of finite differences used, at that time, a simple continuum approach, which showed rapidly its limitations when simulating karst aquifers (BONNET, MARGAT & THIERY 1976).

Finite difference models became interesting again in the late 1980s when used with the double continuum approach (TEUTSCH 1988, LANG 1995, MOHRLOK 1996).

The first attempt to apply the combined discrete channel and continuum approach to karst aquifers by using a 2-D finite element model (with 1-D karst channels) was made, very probably, at the Centre d'Hydrogéologie de Neuchâtel (CHYN), in the framework of an industrial project ("Simulation du bassin de l'Areuse", an unpublished report of CHYN, 1973). A brief summary of these reports was published later by KIRALY & MOREL (1976a) and KIRALY (1984). A computer code allowing for the association of one-, two- and three-dimensional quadratic elements was achieved in the late 1970s (KIRALY 1979, 1988). It was successfully applied to industrial projects (KIRALY 1985), to research work and was submitted to severe and several verification tests under the international HYDROCOIN project (OECD 1988).

In the 1990s, the combined discrete channel, discrete fracture and continuum approach was applied by WOLLRATH & HELMIG (1991), HELMIG (1993) and MOHRLOK (1996) at a local scale.

2.2. An "ancestor": the Areuse model

The basin of the Areuse spring (128 km^2 in the Jura mountains, Switzerland, with about 1000 mm/year of infiltration) is composed of two karst synclines: the syncline of Brévine and the syncline of Verrières, separated by an underground, impervious anticline threshold at the Bois de l'Halle (figure 1a). Groundwater flows from the Brévine syncline, over this threshold towards the Verrières syncline and the rapidly reacting Areuse spring (mean discharge: 4.6 m^3/s, with peaks of more than 30 m^3/s). More than 200 hydraulic conductivity measurements were carried out in five deep boreholes. The measured values ranked from 10^{-7} to 10^{-6} m/s.

The discharge of the Areuse River, issued from the Areuse Spring, is very low during recession periods (less than 1 m^3/s). In the early seventies it was projected to regulate the river discharge by increasing its discharge at low water stage.

The project was defined as follows. A drainage gallery had to be dug through the threshold of Bois de l'Halle into the Brévine syncline. During recession periods of the Areuse spring, the gallery is opened and water is drained from the Brévine syncline in such a way, that the sum of the natural spring discharge Qs and the discharge of the gallery Qg gives a more or less constant ("regulated") discharge Qr=Qs+Qg=const. Taking out groundwater from the Brévine syncline would lower the groundwater level, decrease the natural spring discharge and eventually cut the syncline completely from the Areuse spring. The aim of the model was to simulate the evolution of Qs and Qg for the various values of the regulated discharge Qr and Qg for different periods of drought, with automatic changes of the boundary conditions (gallery open or closed, threshold of Bois de l'Halle open or closed; for more details see KIRALY and MOREL 1976a, KIRALY 1984).

2.2.1. HYDRAULIC CONDUCTIVITIES

TRIPET (1972) had already simulated the Areuse basin with a 2-D electric analog (single continuum) and had to use a hydraulic conductivity of about 10^{-3} m/s for the equivalent con-

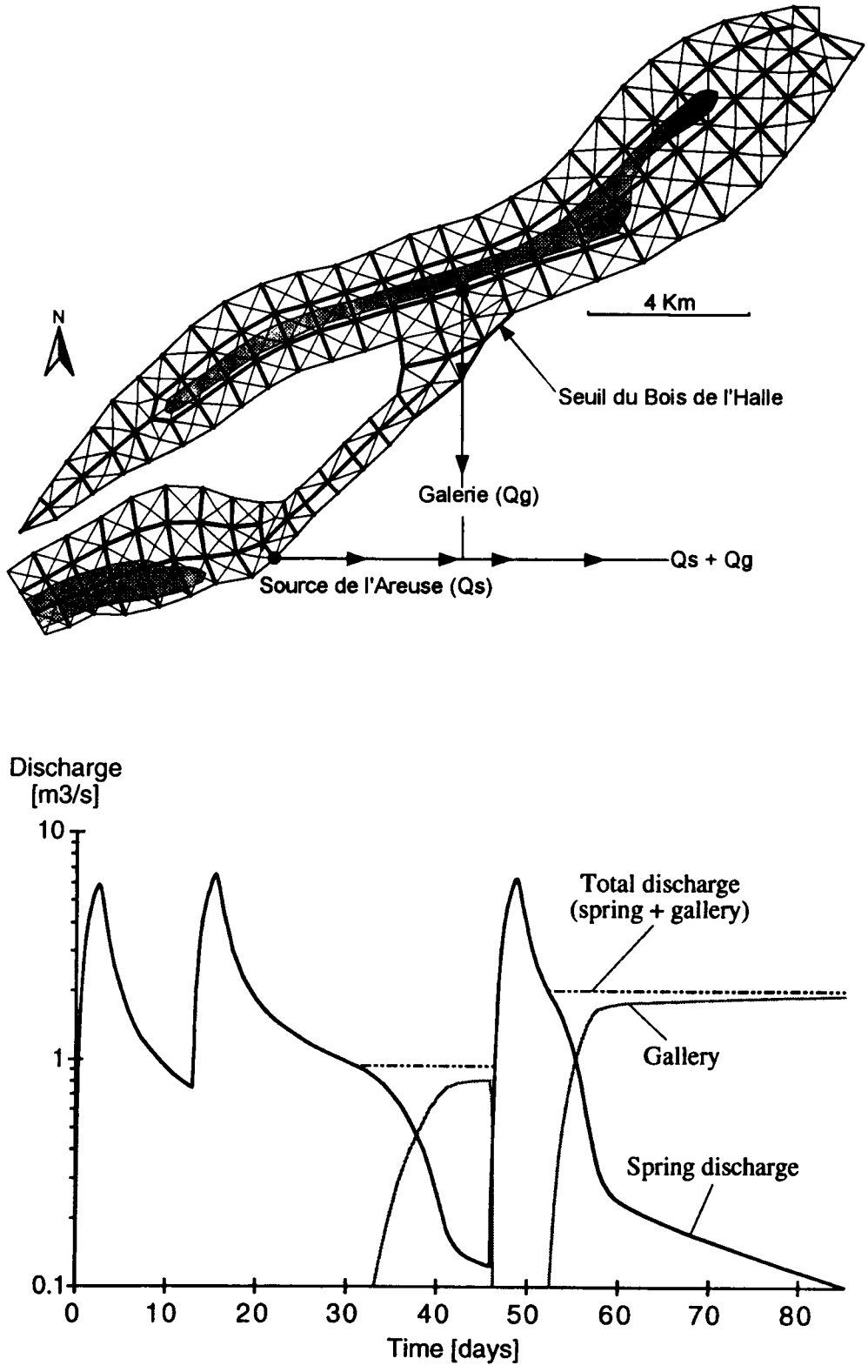

Figure 1: (a) Finite element network for the Areuse model; (b) Example of hydrographs simulated by the Areuse model (KIRALY & MOREL 1976a).

tinuum in order to correctly simulate the hydraulic heads for the given infiltration rate. This is about 3000 times higher than the measured values. This contradiction between measured and model values is due to the *scale effect* of the karst channel network (KIRALY 1973), which was not observed in the boreholes. Evidently enough, the typical karst spring hydrograph could not be simulated with the simple continuum approach.

The contradiction disappeared with the introduction of a fictitious, high conductivity channel network (simulated by 1-D elements) in a low conductivity ($5 * 10^{-7}$ m/s) 2-D continuum representing the fractured limestone volumes (figure 1a). Nearly the whole aquifer volume had a very low hydraulic conductivity, however the global structure behaved as a highly transmissive system. Qualitatively it was the right type of structure: we were not very far from karst! We got even closer to karst with the infiltration problem.

2.2.2. INFILTRATION

The chosen spacing of the karst channels (more or less 1 km) allowed to simulate correctly the exponential part of the recession curve of the Areuse spring (see figure 1b). The correct simulation of the peak-flow and the rapidly decreasing non-exponential part of the recession curve required, however, that more than 60% of the infiltration arrive in "concentrated" form, directly into the high conductivity channels. The concentrated infiltration in the model must have a physical counterpart in the real system. A sound hypothesis would be to suppose, that beside some small rivers disappearing in swallowholes in the Brévine valley, an important part of the infiltration is drained rapidly, probably already at shallow depth in a thin high conductivity layer, towards the karst channel network and the karst spring. This would be the epikarstic zone defined by MANGIN (1975).

2.2.3. CONSEQUENCES OR BACK TO THE REAL SYSTEM

The concentrated infiltration incorporated into the FE model had another consequence, which was investigated more in detail by KIRALY & MOREL (1976b): the inversion of gradients between the high conductivity channels and the low conductivity volumes. The model showed that during recharge periods the simulated hydraulic heads have a higher value in the channels than in the low permeability volumes. That means, karst channels do not drain, but inject water into the fractured volumes. During recession periods the situation is reversed: the simulated hydraulic heads have a lower value in the high conductivity channels, which drain the low conductivity volumes (as it should be).

The inversion of gradients between the simulated karst channels and fractured volumes is produced only by important concentrated infiltration and the phenomenon is, perhaps, not so general as it was supposed by SCHOELLER (1967). This is particularly interesting, because the variation of the hydraulic heads and the inversion of gradients represent the *experimentally verifiable consequences* of our hypotheses on the infiltration and groundwater flow mechanisms in karst aquifers. They suggest to go back to the real system and check them by observing the hydraulic heads *separately* in the high conductivity channels and the low conductivity volumes.

2.2.4. TODAY'S POINT OF VIEW

From a purely "technical" point of view (i.e. from the point of view of numerical analysis) the Areuse model was a bad model. The discretization in finite elements was not fine enough, there was no proof of convergence for the solution, in a 2-D model the 1-D elements do not really simulate pipes but trenches, etc. From a hydrogeological point of view the Areuse model was not so good, either:

- the fictitious karst network had probably nothing to do with the real karst channel geometry (excepting perhaps an equivalent density);
- the piezometric "towers" appearing in 2-D models (see figure 2) have not much to do with the form of the real water table (but their mean altitudes are right);
- the 2-D approximation does not allow to simulate the vertical variation of the hydraulic heads, etc.

From a heuristic point of view, however, it was a very good model. Even if in a very simplified and naive form, the Areuse model had the most important properties of a karst aquifer (duality of the hydraulic conductivity field, duality of the infiltration processes, duality of the groundwater flow field, concentrated discharge at the karst spring). The problems we met with the Areuse model were actually relevant to the study of karst aquifers and suggested further investigations on the theoretical level, as well as in the domain of empirical field works. A few of these subjects are:

- exchange phenomena between low conductivity volumes and karst channels (both groundwater flow and transport);
- concentrated and diffuse infiltration: their effect and relative importance;
- vertical variation of hydraulic heads in karst aquifers, occurrence of the inversion of gradients;
- checking the interpretations obtained by the hydrograph separation methods applied to karst springs;
- effect of the epikarst on the concentrated infiltration (simulation by 3-D models).

2.3 A 3-D approach: the Epikarst model

2.3.1. AIM OF THE MODEL

As mentionned above, earlier numerical experiments with 2-D finite element models showed the necessity to impose a high proportion of concentrated infiltration in order to generate the typical "karstic" storm hydrographs (KIRALY & MOREL 1976a, 1976b). It was supposed, that beside the rivers disappearing in sinkholes, the concentrated infiltrations would result from the rapid drainage in a high permeability "skin" at shallow depth: the epikarst (MANGIN 1975). However, the epikarst layer could not be explicitely included in these 2-D models. To indirectly show its role, we explicitely introduced the epikarst layer in a "synthetic" 3-D finite element model and varied the proportion of the diffuse infitrations with respect to the concentrated infiltrations resulting from the rapid drainage in the epikarstic zone. As the model is transparent for the modeller, the behaviour of the theoreti-

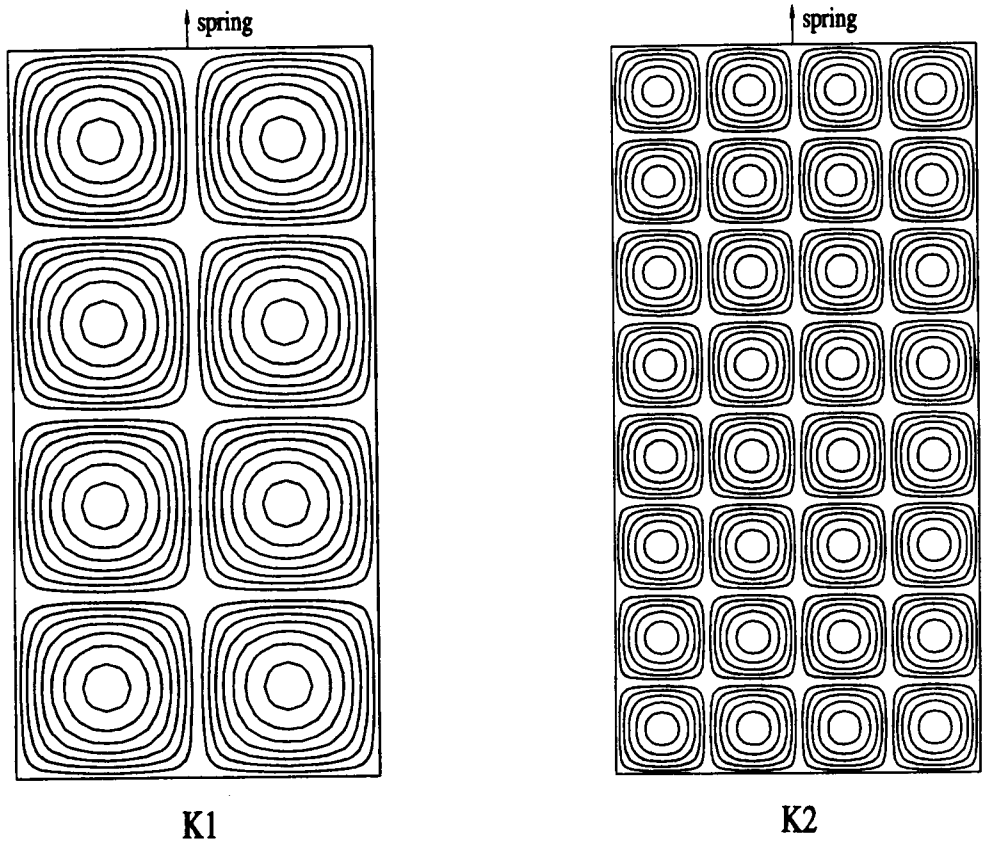

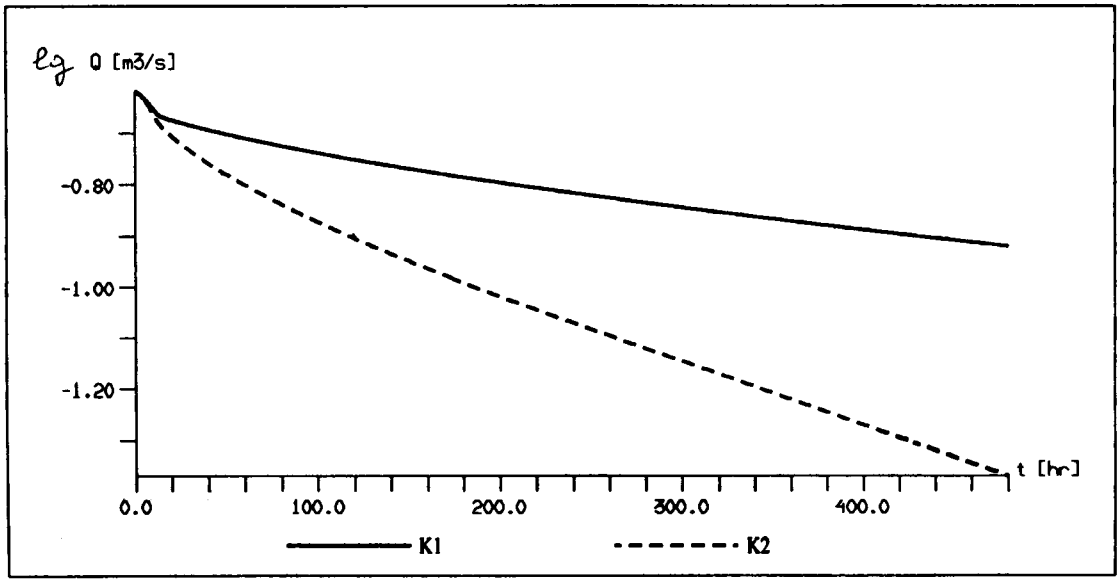

Figure 2: Effect of the density of the high conductivity drainage network on the recession curve of karst springs. Hydraulic conductivities, storativities, infiltration rates and model areas are the same in both cases (after Kiraly, lecture notes).

theoretical karst aquifer can clearly show the effect of epikarst on the spring hydrograph, on the baseflow component of the spring discharge, on the variation of hydraulic heads and fluxes during recharge and recession periods, as well as on the recharge conditions of the low permeability fractured volumes. The detailed results of this study are presented in KIRALY, PERROCHET & ROSSIER (1995). Here we show only a few diagrams without many comments.

2.3.2. BRIEF DESCRIPTION OF THE "SYNTHETIC" KARST AQUIFERS

The diagram of figure 3a shows the 3-D geometry of a theoretical "half-syncline" drained by a very simplified high-permeability karst channel network. The karst channels are simulated by quadratic 1-D elements introduced "in sandwich" between the quadratic 3-D elements simulating the low-permeability fractured volumes.

Diagrams 3b and 3c show a steady state solution without epikarst and the drastic contrast between the rather "gentle" groundwater table and the complexity of the potential distribution in the interior of the aquifer. As a matter of fact, the knowledge of the only groundwater table would not give any information on the flow processes and on what happens in the interior of the aquifer. Note that nearly the entire volume of the mean aquifer (including the high-permeability channel network) is *below the karst spring level*, in the saturated zone.

The epikarst is simulated by a 2-D finite element layer, which will discharge into the channel network of the 3-D syncline, such as represented in figure 4. The hydraulic heads are imposed at the base of the epikarst model (where the channels intersect the 2-D layer), and the calculated discharges are injected at each time-step into the channel network of the 3-D model. This will represent the *concentrated infiltration function* for the mean aquifer.

Figure 5 represents a small "shallow" karst aquifer with an important vertical exaggeration. The aquifers of this type generally develop on plateaus or gently dipping cuestas. In the theoretical aquifer represented in figure 5, the karst network is located above the spring level and is *unsaturated* everywhere. The channels are actually *underground rivers* and represent seepage surfaces with variable boundary conditions for the low-permeability fractured volumes. The free groundwater table was obtained by simulating the steady-state, saturated/unsaturated flow in the low-permeability volumes. The detailed results of the transient simulations will be presented in another paper.

The karst syncline described above and the shallow karst of figure 5 represent two extremes and their reaction to important concentrated infiltrations will not be the same. The aim of including the "shallow karst" configuration in this paper is to remind the reader of the diversity of karst aquifers and to avoid abusive generalization of the results obtained by the saturated karst syncline model.

2.3.3. HYDRAULIC CONDUCTIVITY, STORAGE COEFFICIENT AND INFILTRATION

The hydraulic parameters are the same for all variants of the epikarst model. The hydraulic conductivities K are realistic: $5 * 10^{-6}$ [m/s] for the low-permeability fractured volumes and

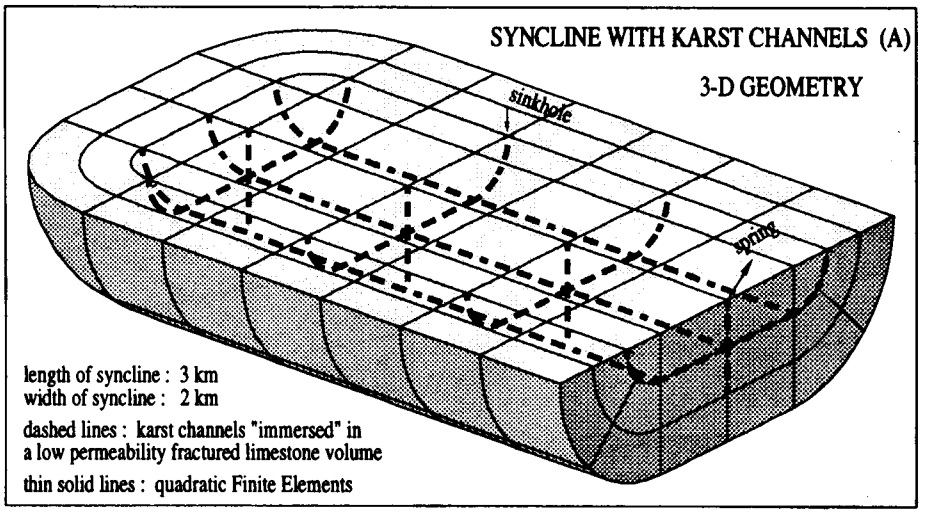

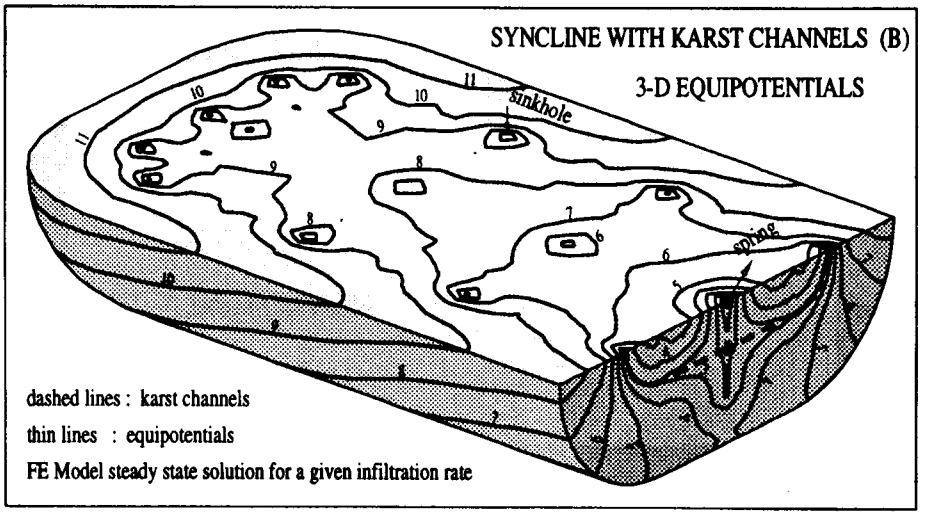

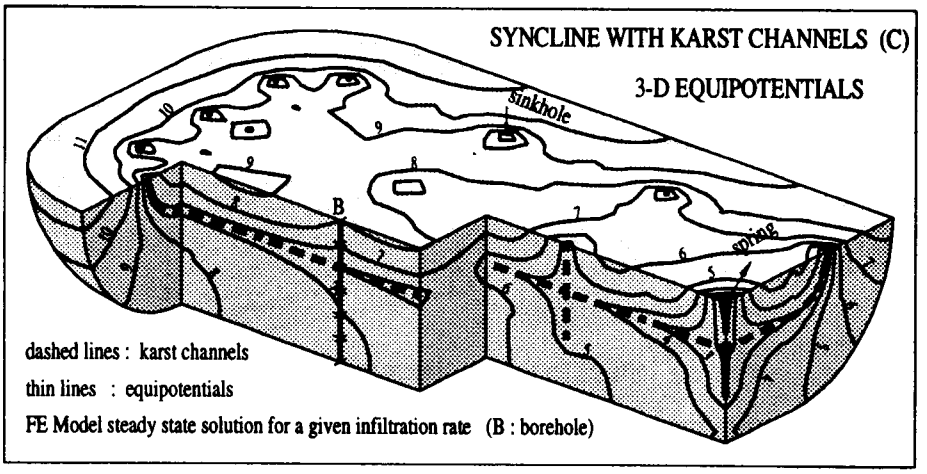

Figure 3: Finite element model for a theoretical karst syncline.

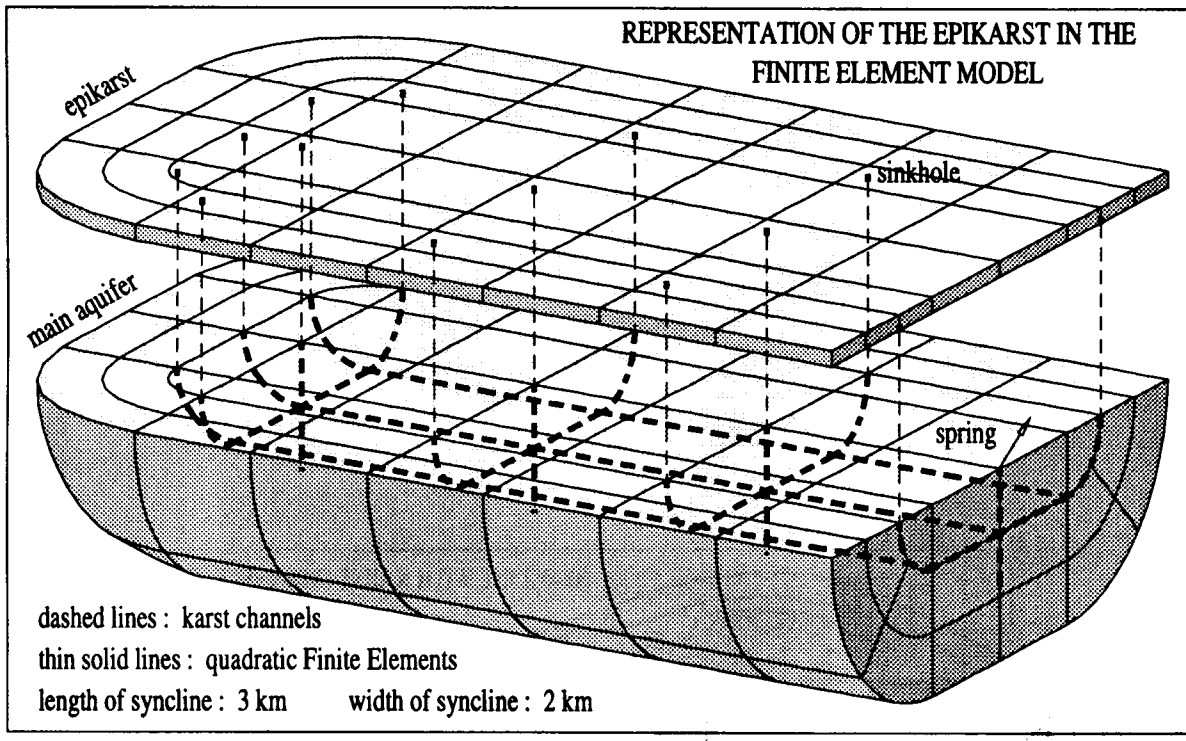

Figure 4: Representation of the epikarst in the finite element model.

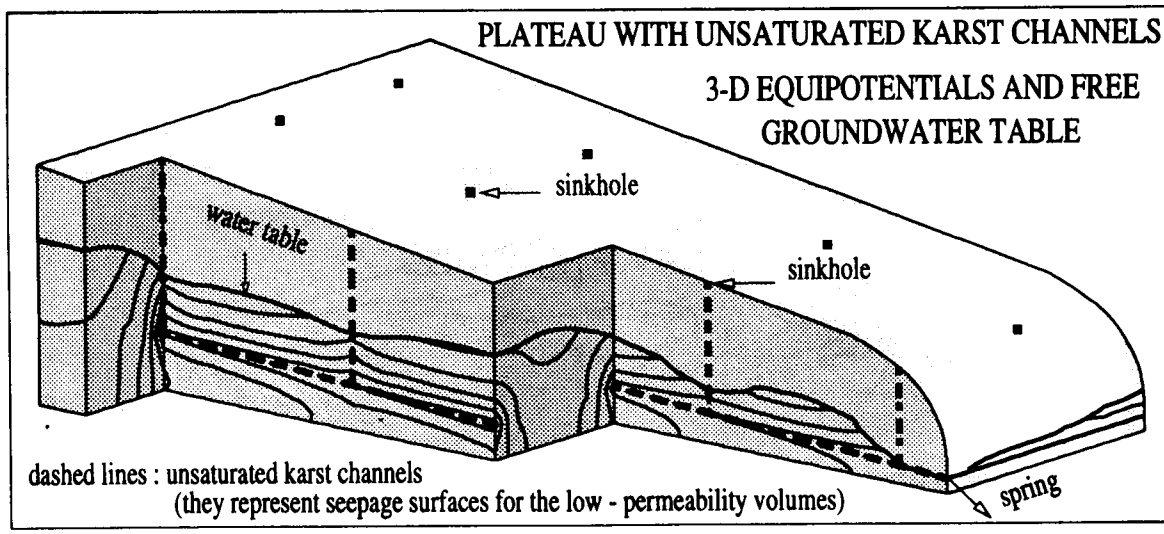

Figure 5: Shallow karst aquifer model, with unsaturated karst channels.

10° [m/s] for the high-permeability karst channels. In the 2-D epikarst layer the transmissivity T is relatively high: about 5 * 10^{-2} m^2/s. Linear Darcy's law is used throughout the models. The specific storage coefficients S_S are kept artificially low in order to "accelerate" the evolution of the simulated hydraulic head and flow field. In the channel network the values of S_S are 400 to 500 times higher than in the low-permeability fractured volumes.

Finally it must be emphasized that we use in both models a very simplified karst channel network. In real systems the karst network is hierarchically organized, with lower and higher order branches having lower and higher hydraulic conductivity values. In the above described models all branches of the karst network are of the same order of magnitude and have the same hydraulic conductivity.

The volume of the total infiltrations remains the same in each variant, but the proportion of the diffuse and concentrated infiltrations will change from one variant to another. Four cases have been simulated:

- DSYN0 : 100% diffuse infiltration 0% drained by the epikarst
- DSYN20 : 80% diffuse infiltration 20% drained by the epikarst
- DSYN50 : 50% diffuse infiltration 50% drained by the epikarst
- DSYN100 : 0% diffuse infiltration 100% drained by the epikarst

Figure 6 represents the total recharge function of the epikarst and the concentrated recharge function of the karst channels for variant DSYN100. There are three input events ("storms"), of a duration of 24 hours each. During the first and second event the infiltrations are distributed over the whole syncline. During the third "storm", infiltration takes place only on a small stripe in the middle part of the model, representing about 30% of the total infiltration area.

2.3.4. EFFECT ON THE SHAPE OF THE SPRING HYDROGRAPH

Figure 7 is self-explanatory: it represents the spring hydrographs for different proportions of infiltration drained by the epikarst into the high-permeability channel network. It appears clearly that without some kind of concentrated infiltrations we cannot simulate the typical karstic reactions of the spring. The rise of the groundwater table in the low-permeability volumes cannot "press" enough water into the karst channels to cause a typical karstic storm hydrograph at the spring. It seems reasonable to admit that in most "open" karst aquifers more than 40% of the infiltrations should be drained rapidly into the karst channels (also see KIRALY & MOREL 1976a, JEANNIN & GRASSO 1995).

2.3.5. EFFECT ON THE HYDRAULIC HEADS

Earlier numerical experiments with 2-D finite element models suggested that concentrated infiltrations might cause an inversion of the gradients between karst channels and low-permeability volumes (KIRALY & MOREL 1976a, 1976b). These 2-D models cannot show, however, the vertical distribution of the hydraulic heads in a borehole.

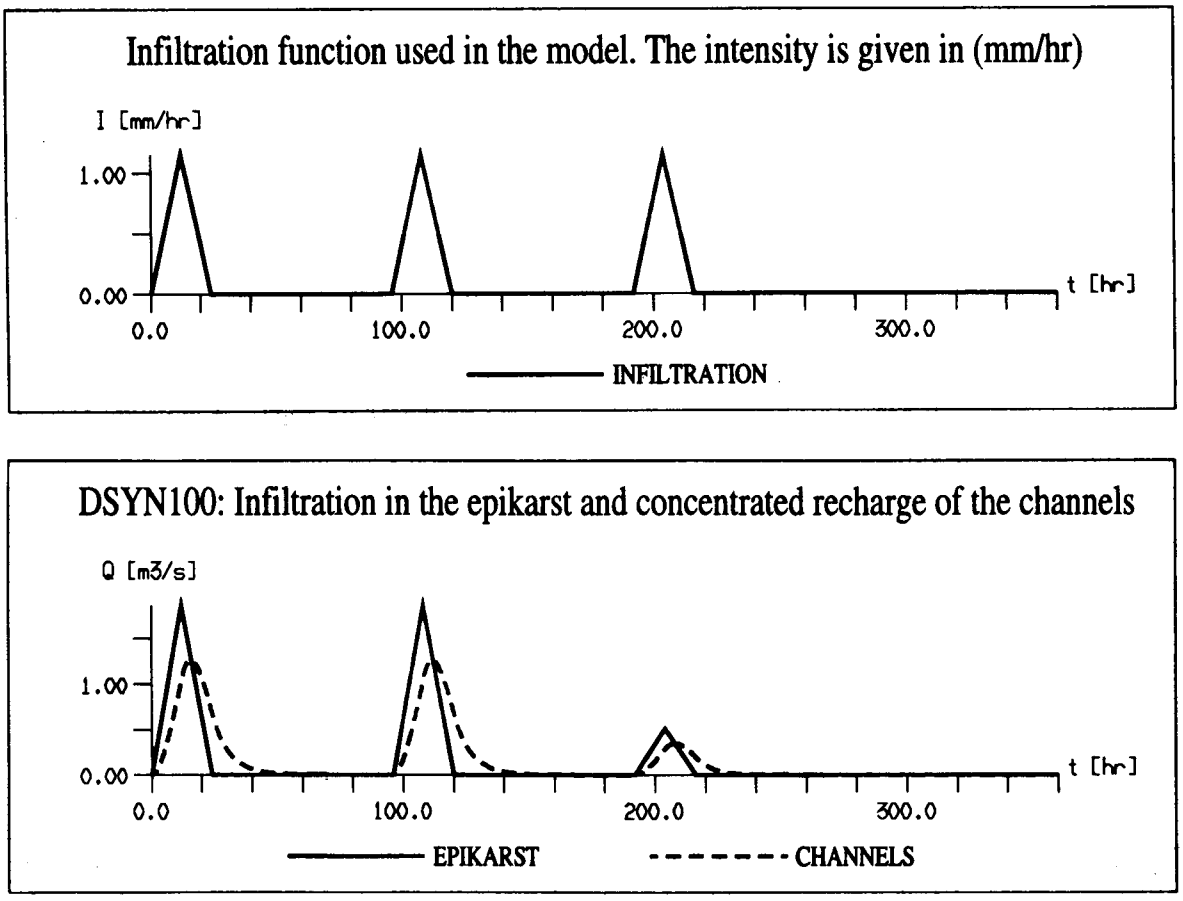

Figure 6: Total recharge function of the epikarst and concentrated recharge function of the karst channels for variant DSYN100.

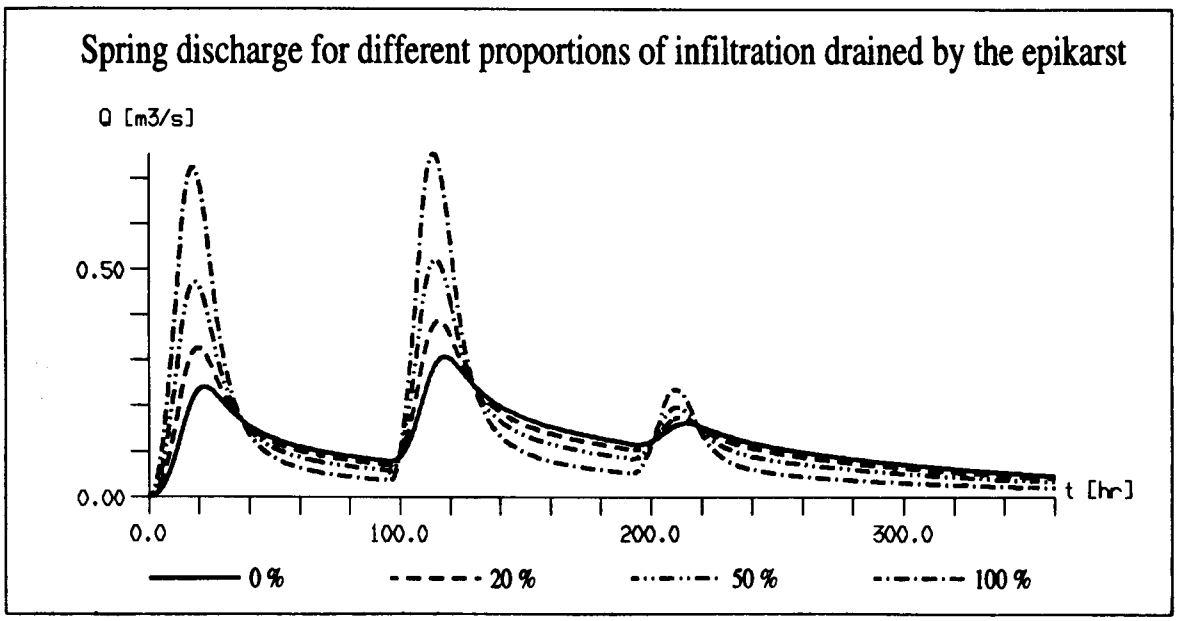

Figure 7: Simulated spring hydrographs for different proportions of infiltration drained by the epikarst.

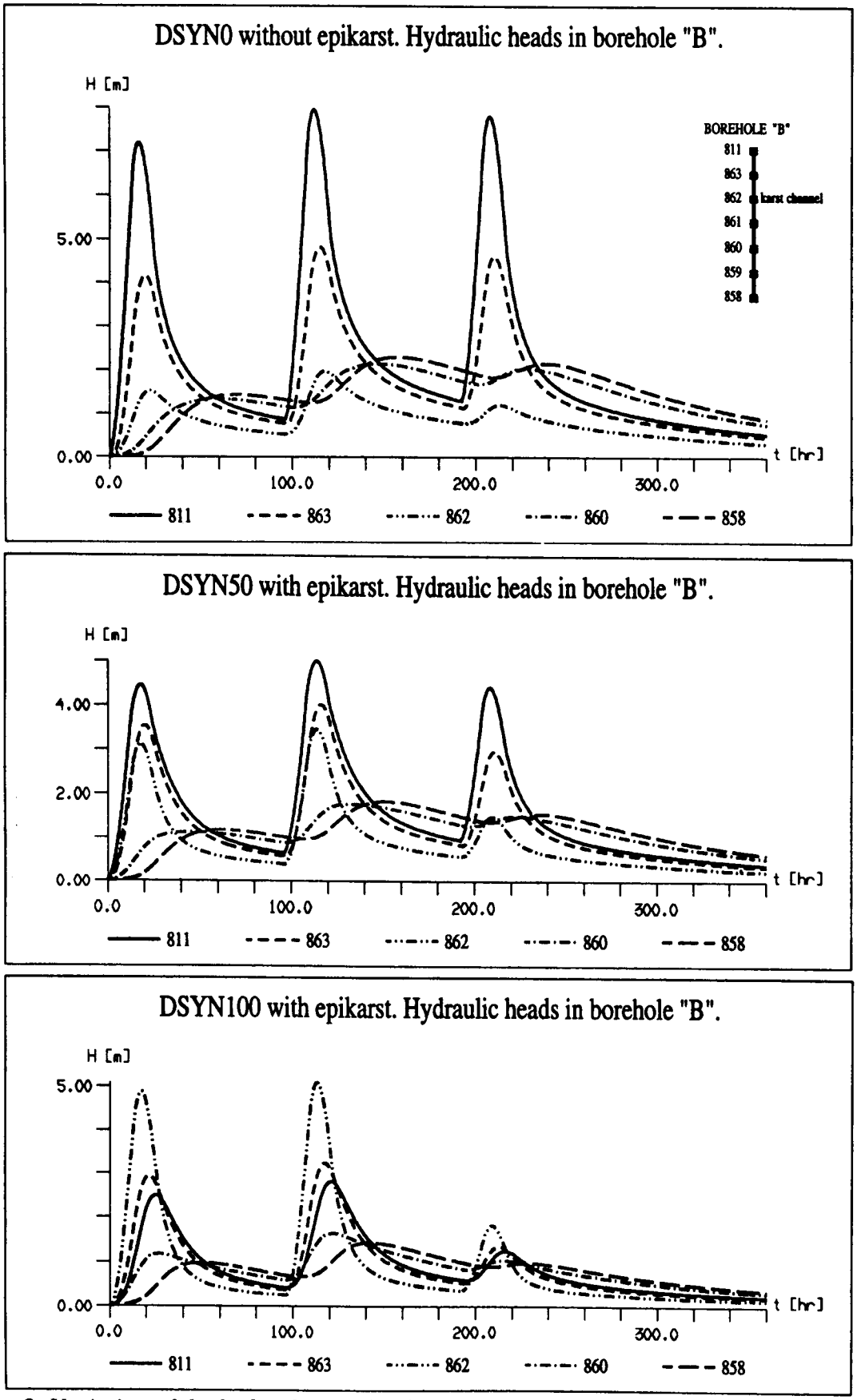

Figure 8: Variation of the hydraulic head in borehole "B" for DSYN0 (a), DSYN50 (b) and DSYN100 (c).

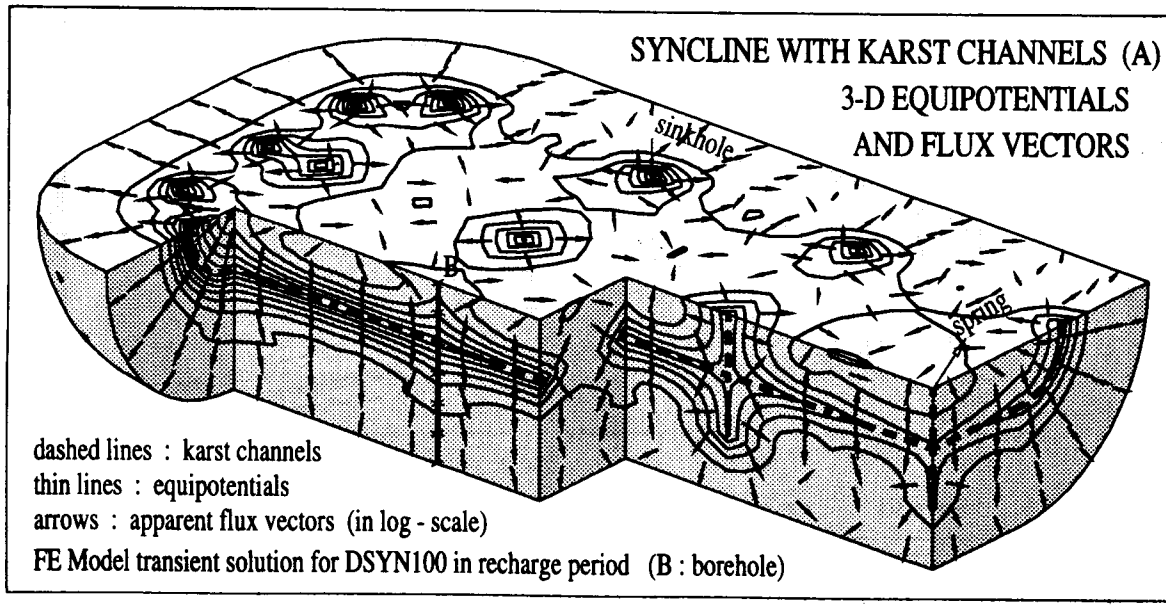

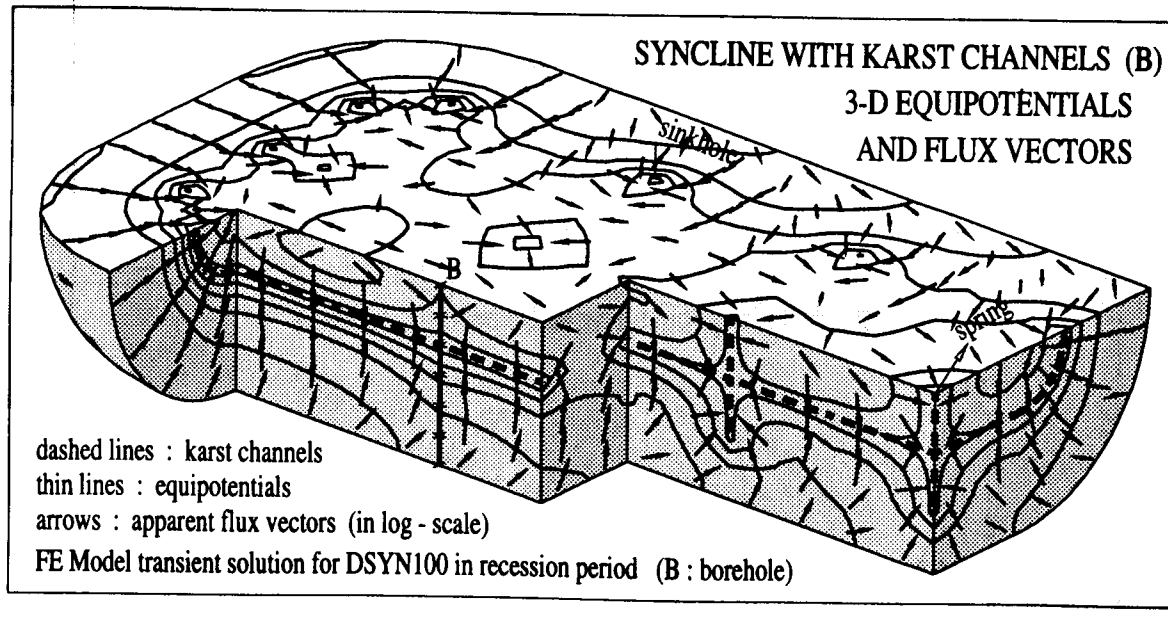

Figure 9: Variation of the hydraulic head for DSYN100, in recharge period (a) and in recession period (b). Location of borehole "B" shown on figure 8.

Taking advantage of the 3-D model, we "registered" the simulated heads in an imaginary borehole "B", the location of which is presented in figure 3c. The borehole intersects a karst channel and the hydraulic heads are measured at seven points between the top and the base of the aquifer.

The results are represented for variants DSYN0 (no concentrated infiltrations, see figure 8a) and DSYN50 (50% of the infiltrations are concentrated, see figure 8b), as well as for the "extreme" variant DSYN100 (100% of the infiltrations are concentrated, see figures 8c, 9a and 9b). Again, the figures are self-explanatory and do not need many comments.

During the recharge period there is nearly always an inversion of gradients between the karst channel and the low-permeability volumes located below the channel. The concentrated infiltrations must be really important to produce the same inversion with respect to the low-permeability volumes located above the channel. The blockdiagrams of figures 9a and 9b clearly show the recharge and drainage mechanism with epikarst and concentrated infiltration.

The practical consequences of these theoretical results are important: *the hydraulic heads should be measured separately in the high-permeability segments and in the low-permeability segments* of boreholes or piezometers. If we measure only one "groundwater level" in an otherwise heterogeneous borehole, the results will be rather misleading than helpful. Other practical consequences are related to the determination of the baseflow component, to the recharge mechanism of the low permeability fractured volumes, to the interpretation of the chemical or isotopic composition of the spring-water, etc.

2.3.6. EFFECT OF THE EPIKARST ON THE "BASEFLOW" COMPONENT OF KARST SPRINGS

In spite of the fact, that the inversion of gradients between karst channels and low-permeability volumes is well known by many karst hydrogeologists, most of the graphically obtained baseflow hydrographs do not show the logical consequence, namely the zero (or negative) baseflow value during recharge periods. One of the few exceptions is found in TRIPET (1972), who suppressed the baseflow component of the Areuse spring during the recharge periods.

Taking advantage of the possibility to calculate the contribution of the low-permeability 3-D elements to the nodes located on the 1-D karst channels, we computed the baseflow component for each variant. The dramatic effect of the concentrated infiltrations on the baseflow component is presented in figure 10 for variants DSYN0, DSYN50 and DSYN100. The appearance of negative baseflow during the recharge period indicates that the karst channels inject more water into the low-permeability volumes than they drain. The volume of this recharge might not be very important, but the fact that the low-permeability volumes may be recharged "from the interior" should not be overlooked.

Another consequence of the negative baseflow appears when estimating the "rapid infiltration" from the spring hydrograph. Generally this is done by substracting the graphically determined baseflow component from the total discharge curve. Now, when the baseflow is negative, it should be added to the spring discharge, otherwise the intensity of the rapid or direct infiltration will be systematically underestimated (see figures 10b and 10c).

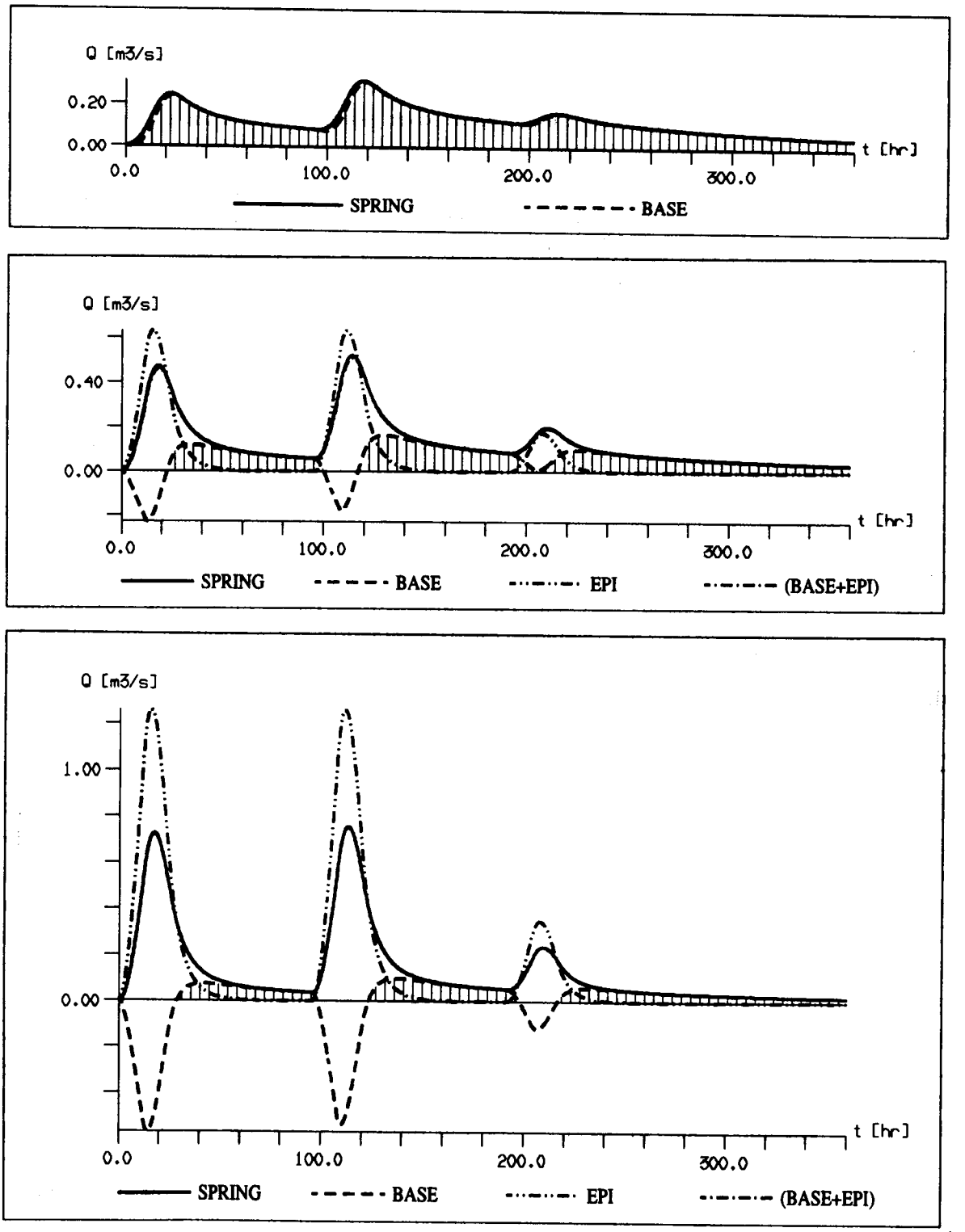

Figure 10: Springflow, baseflow, epiflow and (epiflow + baseflow) for variants DSYN0 (a), DSYN50 (b) and DSYN100 (c). Note that the curve (baseflow + epiflow) is not visible, because it coincides almost exactly with the springflow. Also note, that concentrated infiltration (epiflow) may be greater, or even much greater than the spring discharge.

As the model allows the independent estimation of the baseflow and of the rapid or concentrated infiltration into the karst channel network (which will be called later "*epiflow*"), we can take a critical look at the usually accepted chemical or isotopic hydrograph separation methods.

Figures 10b and 10c show, that the "new water component" obtained by the End Member Mixing Analysis (EMMA) could not be identified with the "rapid recharge to the conduit system after a storm", as it was stated by DREISS (1989, page 121). Indeed, the "new water component" obtained by EMMA must be always smaller than the spring discharge, but figures 10b and 10c indicate clearly that the rapid recharge into the karst channels, noted as the epiflow, may be greater (or even much greater) than the spring discharge.

2.3.7. REMARKS ON THE RECHARGE OF THE LOW CONDUCTIVITY VOLUMES: THE "FARADAY CAGE" EFFECT OF EPIKARST

The huge low permeability fractured limestone volumes are often designated as the capacitive part of karst aquifers. They might contain important groundwater resources, and their recharge mechanism may have important practical consequences on the groundwater management problems (baseflow of karst springs, exploitation of groundwater by pumped wells or galleries, etc.).

Figure 4 (deep karst type syncline) and figure 5 (shallow karst type) suggest that a well developed epikarst layer enhancing the concentrated infiltration into the high conductivity karst channel network will short-circuit the low conductivity volumes and will play the role of a Faraday cage with respect to the main aquifer. Depending on the importance of this Faraday cage effect, the recharge of the low conductivity volumes could be much smaller than in the case of pure diffuse infiltration, with the above mentioned important consequences on the groundwater management problems. In the deep syncline configuration the inversion of gradients will always contribute to recharging the low conductivity volumes "from the interior", but in the shallow karst configuration the short-circuit of the low permeability volumes might be almost total.

3. Conclusions and outlook

Karst aquifers are 3-D systems and cannot be reduced to 2-D objects without loosing important informations on the infiltration processes and the distribution of hydraulic heads. Numerical experiments with a 3-D finite element model using the combined discrete channel and continuum approach, and simulating the infiltration and groundwater flow processes in a highly simplified theoretical karst aquifer, allowed to show the importance of the existence or non-existence of an epikarst zone enhancing concentrated infiltration. The effect of the epikarst on the hydraulic head and the groundwater flow field has practical consequences on the monitoring strategies applied for karst aquifers, on the interpretation of the global responses obtained at the karst springs and on the estimation of the recharge of the low conductivity capacitive volumes. Hydraulic head measurements should always be

related to zones of known hydraulic conductivity and the "piezometric maps" of karst aquifers should always indicate the hydraulic conductivity at the measurement points (see, for example, JEANNIN 1995).

Future research is needed in the simulation of transient, turbulent flow at a basin-wide scale, using the discrete channel and continuum approach. The comparison of a spring hydrograph simulated with turbulent channel flow, and another spring hydrograph simulated with linear channel flow would certainly improve the interpretation of empirical karst spring hydrographs.

Acknowledgements

Some of the computer codes used for the groundwater flow simulation and some of the ideas presented in this paper were developed in the framework of earlier research projects supported by the Swiss National Foundation for Scientific Research. Our most sincere thanks to this institution.

P.-Y. Jeannin and A. Grasso have been spending much time on the verification of different types of model results in real aquifers. We thank them for the discussions and for the work carried out in the field.

M. Bouzelboudjen and P.-Y. Jeannin refreshed some of the figures. Thanks to them for their help.

References

BEDINGER M.S. 1966. Electric analog study of cave formation. Nat. speleol. Soc. Bull. Vol. 28, No 3: 127-132.

BONNET M., MARGAT J. & THIERY D. 1976. Essai de représentation du comportement hydraulique d'un système karstique par modèle déterministe: application à la « Fontaine de Vaucluse ». Deuxième colloque d'hydrologie en pays calcaire, Annales scientifiques de l'Université de Besançon, fasc. 25, 3e série: 79-95.

CHYN 1973. Bassin de la source de l'Areuse. Etude de la régularisation de l'Areuse par modèle mathématique. – Unpubl. report, Centre d'hydrogéologie, Université de Neuchâtel.

DREISS S.J. 1989. Regional scale transport in a Karst aquifer: 1. Component separation of spring flow hydrographs. Water Resources Research, Vol. 25, 1: 117-125.

HELMIG R. 1993. Theorie und Numerik der Mehrphasenströmungen in geklüftet-porösen Medien. Institut für Strömungsmechanik und Elektron. Rechnen im Bauwesen der Universität Hannover, Bericht Nr 34/1993, 186 p.

IRONS B. M. 1970. A frontal solution program for finite element analysis. Int. Journ.Num. Math. Eng., 2: 5-32.

JEANNIN P.-Y. & GRASSO A. 1995. Recharge respective des volumes de roche peu perméable et des conduits karstiques, rôle de l'épikarst. Bulletin d'Hydrogéologie, 14: 95-111.

JEANNIN P.-Y. & MARÉCHAL J.-C. 1995. Lois de pertes de charge dans les conduits karstiques: base théorique et observations. Bulletin d'Hydrogéologie, 14: 149-176.

JEANNIN P.-Y. 1995. Comportement hydraulique mutuel des volumes de roche peu perméable et des conduits karstiques: conséquences sur l'étude des aquifères karstiques. Bulletin d'Hydrogéologie, 14: 113-148.

KIRALY L. 1973. Notice explicative de la carte hydrogéologique du canton de Neuchâtel. Supplément au Bulletin de la Société neuchâteloise des sciences naturelles, Tome 96, 16 p. + carte.

KIRALY L. 1975. Rapport sur l'état actuel des connaissances dans le domaine des caractères physiques des roches karstiques. In: A. BURGER & L. DUBERTET (eds), Hydrogeology of karstic terrains, Int. Union of Geol. Sciences, B, 3:53-67.

KIRALY L. & MOREL G. 1976a. Etude de régularisation de l'Areuse par modèle mathématique. Bulletin du Centre d'Hydrogéologie, 1: 19-36.

KIRALY L. & MOREL G. 1976b. Remarques sur l'hydrogramme des sources karstiques simulé par modèles mathématiques. Bulletin du Centre d'Hydrogéologie, 1: 37-60.

KIRALY L. 1978. La notion d'unité hydrogéologique. Bulletin du Centre d'Hydrogéologie, 2: 83-216.

KIRALY L. 1979. Remarques sur la simulation des failles et du réseau karstique par éléments finis dans les modèles d'écoulement. Bulletin du Centre d'Hydrogéologie, 3: 155-167.

KIRALY L. 1984. Régularisation de l'Areuse (Jura suisse) simulée par modèle mathématique. in: A. Burger & L. Dubertret (eds), Hydrogeology of karstic terrains. Case histories., International Contributions to Hydrogeology, No 1: 94-99.

KIRALY L. 1985. FEM301 - A three dimensional model for groundwater flow simulation. NAGRA Technical Report 84-49, 96 p.

KIRALY L. 1988. Large scale 3-D groundwater flow modelling in highly heterogeneous geologic medium. In: E. CUSTODIO *et al.* (eds), Groundwater flow and quality modelling, 761-775, NATO ASI series, 224.

KIRALY L., PERROCHET P. & ROSSIER Y. 1995. Effect of the epikarst on the hydrograph of karst springs: a numerical approach. Bulletin d'Hydrogéologie, 14: 199-220.

LANG, U. 1995. Simulation regionaler Strömungs- und Transportvorgänge in Karstaquiferen mit Hilfe des Doppelkontinuumansatzes: Methodenentwicklung und Parameterstudie. Ph.D. thesis, Institut für Wasserbau, Universität Stuttgart, 179 p.

MANGIN A. 1975. Contribution à l'étude hydrodynamique des aquifères karstiques. Thèse de doctorat, Université de Dijon, 124 p.

MOHRLOK U. 1996. Parameter-Identifikation in Doppel- Kontinuum-Modellen am Beispiel von Karstaquiferen. Dissertation an der Geowissentschaftlichen Fakultät der Universität Tübingen, TGA, Reihe C, 31, 125 p.

OECD 1988. The International HYDROCOIN Project. Level 1: code verification. OECD Publications, Paris, 198 p.

SCHOELLER H. 1967. Hydrodynamique dans le karst. Chronique d'Hydrogéologie, 10: 7-21.

TEUTSCH G. 1988. Grundwassermodelle im Karst: Praktische Ansätze am Beispiel zweier Einzugsgebiete im Tiefen und Seichten Malmkarst der Schwäbischen Alb. Ph.D. thesis, Universität Tübingen, 205 p.

TRIPET J.-P. 1972. Etude hydrogéologique du bassin de la source de l'Areuse. Mat. carte géol. de la Suisse, série Hydrologie, 21, 183 p.

TRÖSCH J. & ZURBRÜGG C. 1995. Turbulent flow in high permeable karst. Bulletin d'Hydrogéologie, 14: 235-240.

WOLLRATH J. & HELMIG R. 1991. SM-2, Strömungsmodell für inkompressible Fluide, Theorie und Benutzerhandbuch. Institut für Strömungsmechanik, Universität Hannover, Techn. Bericht 1991.